Clays and Clay Minerals, Vol. 56, No. 2, 190–206, 2008.

DIFFUSION OF Na AND Cs IN MONTMORILLONITE

GEORG KOSAKOWSKI*, SERGEY V. CHURAKOV, AND TRES THOENEN
Paul Scherrer Institut, 5232 Villigen PSI, Switzerland

Abstract—The state and dynamics of water and cations in pure and mixed Na-Cs-montmorillonite as a function of the interlayer water content were investigated in the present study, using Monte Carlo and classical, molecular-dynamics methods. While highly idealized, the simulations showed that the swelling behavior of hetero-ionic Na-Cs-montmorillonite is comparable to the swelling of a homo-ionic Na- or Cs-montmorillonite. The mixed Na-Cs-montmorillonite is characterized by intermediate interlayer distances compared to homo-ionic Na- and Cs-montmorillonites. Dry, hetero-ionic Na-Cs-montmorillonite is characterized by a symmetric sheet configuration, as is homo-ionic Cs-montmorillonite.

We found that at low degrees of hydration the absolute diffusion coefficient of Cs^+ is less than for Na^+, whereas at greater hydration states the diffusion coefficient of Cs^+ is greater than for Na^+. An analysis of the relative diffusion coefficients (the ratio between the diffusion coefficient of an ion in the interlayer and its diffusion coefficient in bulk water) revealed that water and Na^+ are always less retarded than Cs^+. With large interlayer water contents, tetralayer or more, Na^+ ions preferentially form outer-sphere complexes. The mobility perpendicular to the clay surface is limited and the diffusion is equivalent to two-dimensional diffusion in bulk water. In contrast, Cs^+ ions preferentially form 'inner-sphere complexes' at all hydration states and their two-dimensional diffusion coefficient is less than in bulk water.

The question remains unanswered as to why experimentally derived relative diffusion coefficients of Cs^+ in the interlayer of clays are about 20 times less than those we obtained by classical molecular dynamics studies.

Key Words—Cs^+, Diffusion, Molecular Dynamics, Montmorillonite, Na^+, Swelling, Water.

INTRODUCTION

The retention capability with respect to cations, anions, or neutral molecules such as water opens a wide range of applications for clays as natural or artificial barriers in waste repositories. In many deep geological repositories for radioactive waste, compacted bentonite, mainly composed of Na-montmorillonite, is used to backfill emplacement tunnels (Nagra, 2002). Due to the swelling of the clay material during resaturation of the tunnels, voids are closed. Swelling in combination with the low permeability of the backfill material inhibits the advective transport of radionuclides. In addition, the diffusion of most radionuclides is retarded due to the retention capacity of clay minerals for cations. In an ideal case, the radionuclides are retained in the bentonite buffer long enough to let radioactive decay reduce the radioactive inventory significantly.

In montmorillonite, a sheet of Al octahedra is sandwiched between two sheets of silicate tetrahedra, forming a so-called TOT layer. Montmorillonite crystallites consist of stacks of several TOT layers. Some of the Al^{3+} ions in the octahedral sheets are replaced by cations of lower valence, *e.g.* Mg^{2+}. Similar substitutions are possible in the tetrahedral sheets, where Si^{4+} can be replaced by trivalent cations such as Al^{3+}. These substitutions lead to a negative charge in the TOT layers that has to be compensated by counterions like Na^+ or Ca^{2+} in the interlayer space. The affinity of interlayer cations for water results in uptake of water in the interlayer leading to the characteristic swelling of montmorillonite. Although Na^+ and Ca^{2+} are the most common interlayer ions, they can be exchanged with other cations such as Cs^+ and with organic molecules (Deer *et al.*, 1992).

The state and dynamics of Cs^+ in the interlayer of clay minerals is of special interest, as radioactive Cs isotopes are produced as fission products in nuclear power plants. Radioactive Cs isotopes are present in spent fuel and high-level radioactive waste and have a relatively high mobility in the geosphere. In bulk water, Cs is highly mobile, the diffusivity of Cs is close to that of water, and a factor of ~1.5 greater than for Na (Flury and Gimmi, 2002). The mobility of Cs isotopes in engineered barriers and some host rocks is controlled by their sorption behavior on clay mineral surfaces (Bradbury and Baeyens, 2000).

Classical molecular modeling is a powerful technique for investigation of the structure and the dynamics of water and cations in swelling clay minerals such as montmorillonite, hectorite, or beidellite (Smith, 1998; Kawamura *et al.*, 1999; Greathouse *et al.*, 2000; Chavez-Paez *et al.*, 2001a; Chavez-Paez *et al.*, 2001b; De Carvalho and Skipper, 2001; Hensen and Smit, 2002; Marry and Turq, 2002; Marry *et al.*, 2002a; Arab *et al.*,

* E-mail address of corresponding author:
georg.kosakowski@psi.ch
DOI: 10.1346/CCMN.2008.0560205

2003; Boek and Sprik, 2003; Marry and Turq, 2003; Arab *et al.*, 2004; Ichikawa *et al.*, 2004; Malikova *et al.*, 2004a; Tambach *et al.*, 2004a, 2004b; Skipper *et al.*, 2006). Previous studies modeled the swelling of pure Na-montmorillonite (Boek *et al.*, 1995b; Chavez-Paez *et al.*, 2001b; Marry and Turq, 2002; Marry *et al.*, 2002a; Malikova *et al.*, 2004a) or pure Cs-montmorillonite (Smith, 1998; Marry *et al.*, 2002c) with up to three water layers.

Only a monolayer of water was reported for pure Cs-montmorillonite in experiments and the existence of Cs-montmorillonite with interlayer distances >12.4 Å (equivalent to a monolayer of water) seems questionable (Smith, 1998; Sutton and Sposito, 2001). Sutton and Sposito (2001) investigated the interlayer structure and dynamics in '12.4 Å Cs-smectite hydrates' using Monte Carlo and classical, molecular dynamics simulations. They predicted stable Cs-smectite hydrates at water contents equal to ⅓ and ⅔ of a monolayer. For greater hydration states they were not able to find stable configurations. The self-diffusion coefficient value which they obtained for the interlayer water in Cs-montmorillonite (water content ⅔) was half that of bulk water at standard conditions.

Na- and Cs-montmorillonite were found to have different swelling behaviors. In pure Na-montmorillonite, all hydration states up to three (Mooney *et al.*, 1952; Berend *et al.*, 1995) and four water layers (Norrish, 1954; Pons *et al.*, 1981) have been reported. Greater degrees of hydration and larger interlayer distances are normally viewed as a continuous hydration relating to an unlimited adsorption of water on internal and external surfaces (Brigatti *et al.*, 2006). In general, the one- to four-layer hydrates cannot be considered as defined states in terms of water content and interlayer distance, as these depend on layer charge and relative humidity (Michot *et al.*, 2005; Brigatti *et al.*, 2006).

Marry and Turq (2003) investigated the dynamics of single Cs^+ cations in two types of Na-montmorillonite with water contents corresponding to a bilayer. They found that the diffusion coefficient of Cs^+ is about twice as large as that of Na^+ for the hetero-ionic Otay clay (tetrahedral and octahedral substitutions) and ~1.5 times as large as that of Na^+ for a hetero-ionic Wyoming clay (only octahedral substitutions). Any effects caused by changing the water content were not addressed in this study.

Malikova *et al.* (2004b) investigated the effect of temperature on the diffusion of Na^+ and Cs^+ in homo-ionic montmorillonite clays at low hydration states. In the monolayer case, the diffusion coefficients of Cs^+ were less than those of Na^+. The authors found that the diffusive behavior of water and Na^+ changes towards that of bulk water when moving from monohydrated to bihydrated Na-montmorillonite.

In macroscopic diffusion experiments, the mobility of radionuclides in compacted bentonite or clay-rich rocks is estimated in terms of apparent diffusion coefficients, and effective diffusion coefficients are deduced from additional information on the porosity of the material and sorption of the radionuclides (Van Loon and Jakob, 2005). It should be noted that a comparison of experimental diffusion coefficients and those obtained in classical molecular dynamic simulations is not straightforward. With macroscopic diffusion experiments, it is not possible to investigate directly the interlayer diffusion as in molecular models. Experimental diffusion coefficients represent averaged values over diffusion in the interlayer and diffusion in the complex pore space between the clay platelets. Viewed from a molecular modeling perspective, it is impossible to reproduce the whole complexity of diffusion paths in natural clays with the current models, which are limited to a size which is much less than that of a single clay platelet.

Attempts have been made to derive the macroscopic diffusion behavior based on data from molecular-dynamics modeling, and homogenization analysis (Prayongphan *et al.*, 2006). Bourg *et al*. (2003, 2006) tried to combine experimental data and molecular dynamics results to explain the apparent diffusivity of water, Na and Cs tracers in compacted saturated Na-bentonite. They found much lower relative interlayer diffusion coefficients for Cs tracers derived from experiments compared to the values obtained in molecular dynamics studies. They concluded that this mismatch is caused by the uncertainties in the Cs/clay interaction potentials and in the localization of charge within the clay.

Apart from a few studies, which compared ion diffusion only in mono- or bihydrated states of Na- and Cs-clays by means of molecular modeling simulations (Marry and Turq, 2002; Marry and Turq, 2003; Malikova *et al.*, 2004b), there are no systematic studies of swelling and ion-diffusion in a mixed Na-Cs-montmorillonite. The purpose of this study is therefore to investigate the dynamics of interlayer species of hetero-ionic (mixed Na-Cs) montmorillonite as a function of water content and resulting interlayer spacing, and to determine the dependence of diffusion coefficients of Na^+ and Cs^+ on the interlayer water contents. We performed simulations on a mixed Na-Cs-montmorillonite, with an arbitrary Na-Cs ratio of one as representative of a wider range of mixed montmorillonites, in order to see potential competition effects between Cs^+- and Na^+-diffusion. We think that for a range of Na-Cs compositions, several hydration states can be expected as is the case for pure Na-montmorillonite. The greater hydration states may represent outer surfaces of clay stacks in compacted systems. The detailed evolution of the swelling curve as a function of the Na-Cs composition in mixed montmorillonite is not known.

Finally, note that the model systems discussed are highly idealized, not only in terms of the homogeneity of

the clay layers and the locations of substitutions, but also in terms of hydration. Experimental and modeling studies show that swelling of smectites depends mainly on the kind of interlayer cation (Norrish and Quirk, 1954; Berend *et al.*, 1995; Hensen *et al.*, 2001; Teppen and Miller, 2006), but other factors such as layer charge (Slade *et al.*, 1991; Michot *et al.*, 2005; Laird, 2006) also influence hydration and associated interlayer distances (Ferrage *et al.*, 2005, 2007). In experimental smectite-swelling measurements, a hysteresis is reported (Michot *et al.*, 2005), *i.e.* swelling depends on the direction of the change of water content; it differs in adsorption or desorption experiments. In contrast to the simulations by Hensen and Smit (2002), the method we employed does not permit simulation of such effects. Furthermore, it has been reported that the hydration of the interlayer is not uniform within clays; not only can mixing of bihydrated and trihydrated states in homo-ionic clays occur (Slade *et al.*, 1991; Berend *et al.*, 1995), but interstratifications of bihydrated Ca-montmorillonite and monohydrated Na-montmorillonite layers in a hetero-ionic Ca-Na montmorillonite have also been measured (Iwasaki and Watanabe, 1988). Such effects remain outside the scope of this study. This work focuses on the structure of the water-clay interface and diffusion processes in the interlayer of mixed Na-Cs-montmorillonite.

METHODS OF SIMULATION

System setup

Montmorillonite with a unit-cell composition of $Cat_{0.75}[Mg_{0.75}Al_{3.25}][Si_8]O_{20}(OH)_4$, where *Cat* represents the Na and Cs cations in the interlayer, was investigated. The unit-cell and atomic coordinates of montmorillonite were taken from Skipper *et al.* (1995b). The simulation cell was made up of two TOT layers in the *z* direction and six by four unit cells in the *a* and *b* directions, respectively. The dimensions of a single TOT layer containing 960 atoms were 31.68 Å × 36.56 Å × 6.54 Å. The interatomic distances in the TOT layer were fixed and the layer was treated as a rigid molecule. In the 48 unit cells per simulation cell, 36 of 192 Al atoms in octahedral sites were replaced by Mg^{2+}. The substitution sites were selected to lie as far apart as possible, thereby producing a more regular rather than a random array of Mg atoms (Sainz-Díaz *et al.*, 2002). The positional parameters of the clay structure and the positions of the substitution sites are given in Tables 1 and 2, respectively. The water content was varied systematically from full dehydration to about five layers of water per interlayer. We modeled the pentalayer hydration state which may not exist in reality, in order to assess the change of mobility for interlayer species towards highly hydrated systems. A typical simulation cell therefore contains 1920 clay atoms in two TOT layers, as well as 18 Na^+ ions, 18 Cs^+ ions, and 192 water molecules distributed in two interlayers as shown in Figure 1.

Table 1. Position and charge of the basis sites for constructing a unit cell of the mineral pyrophyllite (dioctahedral 2:1 neutral clay) as reported by Skipper (1995a). From the basis sites, a unit cell of pyrophyllite is constructed by replication through a point inversion at (0.88,0.0,0.0) and conversion to a rhombohedral unit.

Atom	*x* (Å)	*y* (Å)	*z* (Å)	*q* (*e*)
O (surface)	2.64	0.0	3.28	−0.8
O (surface)	1.32	2.28	3.28	−0.8
O (surface)	3.96	2.28	3.28	−0.8
O (OH)	0.0	0.0	1.06	−1.52
H (OH)	0.8815	0.0	1.434	0.52
Si	2.64	1.52	2.73	1.2
Si	5.28	3.05	2.73	1.2
O (apical)	2.64	1.52	1.06	−1.0
O (apical)	5.28	3.05	1.06	−1.0
Mg	−0.88	1.52	0.0	3.0
Mg	−0.88	−1.52	0.0	3.0

The water-water and water-clay interactions were modeled by TIP4P and OPLS force fields (Jorgensen *et al.*, 1983) similar to Boek *et al.* (1995b). Interactions between two sites i and j at a distance r_{ij}, involve Coulomb and Lennard-Jones 6-12 terms,

$$v_{ij}\left(r_{ij}\right) = \frac{q_i q_j}{r_{ij}} - \frac{D_{ij}}{r_{ij}^6} + \frac{E_{ij}}{r_{ij}^{12}} \quad (1)$$

Here, q_i and q_j denote the site charge for sites i and j, and D and E are the Lennard-Jones coefficients, summarized in Table 3. Following Jorgensen and Tirado-Rives (1988), for example, the cross-interaction coefficients are calculated as geometric means of the interaction coefficients from Table 3. The TIP4P-water molecule is characterized by a charge of +0.52*e* placed

Table 2. Positions of the substitutions in the octahedral sheet for one sheet.

x (Å)	*y* (Å)	*z* (Å)
4.4	−1.52	0.0
7.04	6.09	0.0
4.4	16.76	0.0
7.04	24.37	0.0
9.68	28.94	0.0
14.96	1.52	0.0
14.96	10.66	0.0
17.6	15.23	0.0
17.6	21.33	0.0
17.6	30.47	0.0
20.24	7.62	0.0
22.88	33.51	0.0
25.52	1.52	0.0
25.52	10.66	0.0
25.52	19.8	0.0
28.16	24.37	0.0
25.52	28.94	0.0
33.44	12.19	0.0

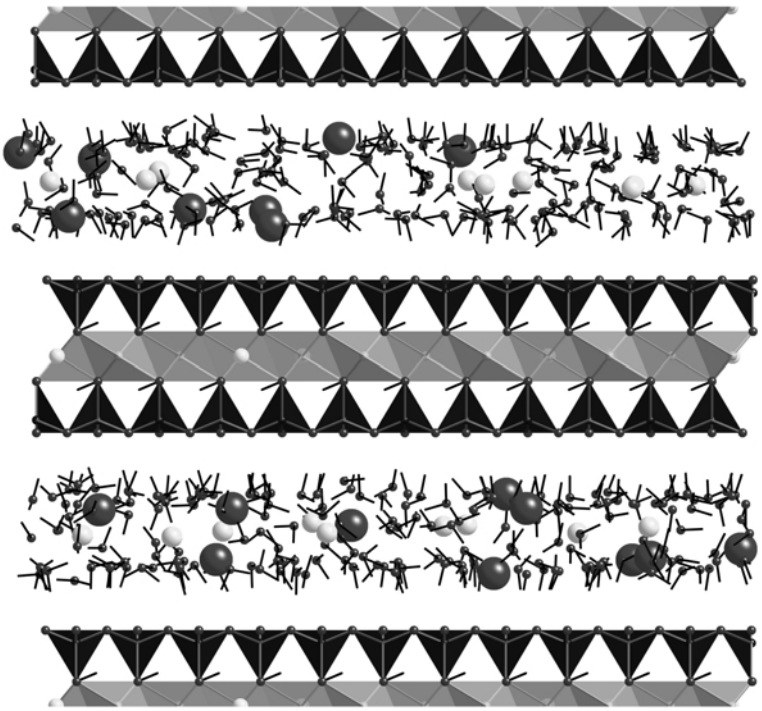

Figure 1. Snapshot from an MD simulation for a typical bilayer system (water contents: 8 water per clay unit, layer spacing: 15.06 Å). The silicon tetrahedra are shown in black; the octahedral sheet in gray; substitutions are light spheres inside the octahedral sheet water OH-groups in the interlayer are shown as sticks; Na^+ cations are smaller light spheres; and Cs^+ cations are bigger, dark spheres.

on each of the two hydrogen sites and a negative charge of $-1.04e$ on a massless charge site, situated at a distance of 0.15 Å along the symmetry axis of the planar water molecule. The fourth site is a neutral oxygen atom that is the only Lennard-Jones interaction site on the molecule. The interaction parameters for Na^+ were adopted from Jorgensen and Tirado-Rives (1988) and the parameters for Cs^+ were taken from Reddy and Berkowitz (1988a, 1988b). Hereafter, this set of interaction parameters is referred to as the OPLS-TIP4P force field. This force field is widely used for the simulation of clay systems (Skipper *et al.*, 1991; Boek *et al.*, 1995a; Skipper *et al.*, 1995a, 1995b; Chavez-Paez *et al.*, 2001a; 2001b; Cygan *et al.*, 2004; Skipper *et al.*, 2006) and is known to work well for the hydration of monovalent ions (see Skipper *et al.*, 2006) for an extended discussion on this topic). The most important restriction of the OPSL-TIP4P force field used is the assumption that each molecule is a rigid body. Considering effects like bond-bending or bond-stretching would require the use of different force fields such as the newly developed CLAYFF molecular model (Cygan *et al.*, 2004).

Table 3. Lennard-Jones parameters used for pair interactions.

	D (Å^6 kcal mol^{-1})	$E \times 10^{-3}$ (Å^{12} kcal mol^{-1})
O–O	610	600
Na–Na	300	14
Cs–Cs	19344	20770.5
Cl–Cl	3500	26000

In the starting configurations, cations and water molecules were placed pseudo-randomly in the interlayer, keeping mass centers apart by at least 1.5 Å. The systems were equilibrated using isothermal-isobaric Monte Carlo simulations (NPT-ensemble) at a temperature of 298 K and a pressure of 0.1 MPa using the code *Monte* (Skipper *et al.*, 1995a). The lattice parameters in the *a*- and *b*-directions were constrained by the geometry of the clay layer and the dimension of the simulation cell was varied in the *z* direction only (perpendicular to the TOT layers). One of the TOT layers was allowed to move within the *a,b* plane, and in the *z* direction, to achieve equilibration of the layer alignment. Equilibration runs were terminated when the oscillations of total energy and layer spacing were normally distributed with constant mean and variance.

Equilibrated systems obtained in the Monte Carlo simulations were taken as starting configurations for the molecular dynamics code DL_POLY (Smith and Forester, 1996; Smith *et al.*, 2002). The molecular dynamics simulations were performed with the same force field parameters as the Monte Carlo equilibration. A Berendsen thermostat was coupled to the system for a

50 ps long initial equilibration phase. The velocities were scaled every 2.5 fs.

Production runs, 500 ps in duration, were performed in the NVE ensemble. The equations of motion were integrated with a time step of 0.5 fs. The molecules and ions in the interlayer were allowed to move freely, whereas the clay sheet atoms remained immobile. The positions of the atoms were recorded every 0.1 ps, from which the average properties were calculated.

Dynamic properties of the interlayer species (diffusion)

Self-diffusion coefficients for ions and water molecules were calculated from the Einstein relationship:

$$D = \lim_{t\to\infty} \frac{\langle r(t)^2 \rangle}{2nt} \quad (2)$$

with the mean-square displacement $r(t)^2$ and $r(t) = R(t) - R(0)$, where $R(t)$ is the particle position at time t. For diffusion in three dimensions $n = 3$. The Einstein relationship can be used to calculate one- or two-dimensional diffusion coefficients. In these cases only movements in one or two directions are considered and $n = 1$ or $n = 2$. For isotropic, non-restricted diffusion, the one-dimensional diffusion coefficients $D_{xx,yy,zz}$ are identical to the three-dimensional diffusion coefficient D_{3D}. In the case of isotropic diffusion within a geometric restriction in one dimension, zz, as in the interlayer of montmorillonite, the one-dimensional diffusion coefficient D^r_{zz} in zz direction approaches zero for infinitely long simulation times. In addition, the two-dimensional diffusion coefficient D^r_{2D} in the xx,yy-plane is converging towards 3/2 D^r_{3D}, where D^r_{3D} is the diffusion coefficient obtained in the restricted medium using the three-dimensional expression from equation 2. D^r_{2D} corresponds to the three-dimensional diffusion coefficient D^r_{3D} in a geometrical, unrestricted medium. For isotropic diffusion, the calculated D^r_{2D} is equivalent to the one-dimensional diffusion coefficients in xx and yy directions $D^r_{xx} = D^r_{yy} = D^r_{2D} = D_{3D}$.

Table 4. D_{exp}: ionic diffusion coefficients measured in electrolytic solutions at 25ºC from Flury and Gimmi (2002). D_{msd}: ionic diffusion coefficients from molecular modeling with 2048 water, 16 Na^+, 16 Cs^+, and 32 Cl^- at a temperature of 298 ± 3 K and a pressure of 1 bar.

Species	D_{exp} ($m^2\ s^{-1}$) × 10^{-9}	D_{msd} ($m^2\ s^{-1}$) × 10^{-9}
Cs^+	2.056	2.0 (±0.1)
Na^+	1.334	1.11 (±0.1)
Cl^-	2.032	2.18 (±0.1)
H_2O	2.3	3.26 (±0.05)

Trajectory length for msd calculations = 10 × 51.2 ps (blocking method).

A "blocking method" (Flyvbjerg and Petersen, 1989) was used to reduce the uncertainty and provide values for the standard deviation of the averaged values. The recorded trajectories are split into several shorter blocks and the average mean-square displacement is calculated.

Diffusion coefficients measured in bulk water can be compared directly to diffusion coefficients from molecular dynamics simulations. This allows validation of the force fields used in the simulations. For this purpose we first calculated diffusion coefficients of Na^+ and Cs^+ (with Cl^- as the anion) from simulations of bulk water (Table 4) and compared them to the experimentally determined values by Flury and Gimmi (2002) derived from electrical conductivity measurements. The simulated system for bulk water was set up as a rectangular simulation cell with periodic boundary conditions that contained 256 TIP4P water molecules, 2 Na^+ and 2 Cs^+. For charge compensation, 4 Cl^- had to be included in the simulation. The Lennard-Jones parameters for Cl^- were adopted from Jorgensen and Tirado-Rives (1988). As described previously, we used isothermal-isobaric Monte Carlo simulations (NPT-ensemble) at a temperature of 298 K and a pressure of 0.1 MPa to equilibrate the system. Unlike the simulations for montmorillonite, the simulations for water require an isotropic pressure regime, *i.e.* all three dimensions of the simulation box were adjusted to match the desired pressure of 0.1 MPa. As in the simulations of the montmorillonites, the equilibrated system was used as a starting configuration for molecular dynamics simulations from which diffusion coefficients and other properties were extracted.

It seems that the diffusion coefficients of Na^+ and Cs^+ in TIP4P-water nearly represent the experimental data, whereas the diffusion coefficient for TIP4P-water is greater than the experimental value. The large water-diffusion coefficient is a known property of the utilized TIP4P force field (Jorgensen *et al.*, 1983). The value obtained in the present study for TIP4P water compares well with the value of ~3.29×10^{-9} $m^2 s^{-1}$ at 25ºC and 1 atm obtained by Mahoney and Jorgensen (2001).

As we are mainly interested in relative changes of mobility in the interlayer compared to bulk water, we use the "relative diffusion coefficient" D_r, defined as the ratio between the two-dimensional interlayer diffusion coefficient and the diffusion coefficient in/of bulk water D_{3D}:

$$D_r = D^r_{2D}/D_{3D} \quad (2)$$

Note that the relative diffusion coefficient used, *e.g.* by Bourg *et al.* (2003, 2006) for the comparison of water and tracer diffusion in highly compacted clays with diffusion in bulk water, has a slightly different definition, as it contains the three-dimensional interlayer diffusion coefficient. We prefer the definition of equation 2, as it allows direct interpretation of the relative diffusion coefficient as a retardation factor for diffusion within the interlayer plane.

RESULTS

Swelling curve for Na-Cs-montmorillonite

The dependence of the interlayer spacing of mixed Na-Cs-montmorillonite on water content is summarized in Figure 2. The simulations clearly show a plateau for a monohydrated state (4−5 H_2O per clay unit cell) and less clearly for the bihydrated state (8−10 H_2O per clay unit cell). Typically, Monte Carlo simulations converge to the mean interlayer distances with variations of ~±0.5 Å.

In order to compare the hydration of the hetero-ionic montmorillonite with that of homo-ionic montmorillonites, simulations were performed with the same system setup for dry, monohydrated, and bihydrated states of Na- and Cs-montmorillonite (Figure 2). Although hydration states greater than a monolayer have never been observed experimentally, we performed our own calculations for bihydrated Cs-montmorillonite and compared the results with the simulated swelling curves for Cs-montmorillonite from Smith (1998) and Marry *et al.* (2002b) in order to test the force field and the system setup. In addition, the simulation results for the homo-ionic clays will be used below for the interpretation of the hetero-ionic simulations.

The interlayer spacings obtained for Na-montmorillonite of 12.64 Å for 5 H_2O per clay unit, and of 15.0 Å for 8 H_2O per clay unit, match those of earlier studies with the same force field (Boek *et al.*, 1995a; Chavez-Paez *et al.*, 2001b), which are in good agreement with experimental results obtained by Calvet (1973) and Fu *et al.* (1990). The values also correspond well to the measurements by Mooney *et al.* (1952) who reported values of 12.2−12.6 Å for monohydrated and 15.3−15.6 Å for bihydrated Na-montmorillonite, as well as to the 15.4 Å given by Norrish and Quirk (1954) for the bihydrated state.

The interlayer distances of 12.7 Å (4 H_2O per clay unit) and 12.9 Å (5 H_2O per clay unit) obtained in this study for monohydrated Cs-montmorillonite are similar to those obtained in other simulations (Smith, 1998; Marry and Turq, 2002) and correspond well to the X-ray measurements by Mooney *et al.* (1952) who reported a value of close to 12.6 Å. In general we found that the interlayer distance of the mono- and bihydrated mixed Na-Cs-montmorillonite is similar to or slightly less than that for Cs-montmorillonite and greater than that for Na-montmorillonite.

The Monte Carlo simulations of dehydrated Na-Cs-montmorillonite resulted in a layer spacing of 10.9±0.1 Å. This value is greater than the value of 10.4±0.1 Å calculated for homo-ionic, dry Na-montmorillonite and is similar to the value of 10.8±0.1 Å which we obtained for a symmetric, dry Cs-montmorillonite. The latter interlayer distance is also in accord with the modeling-based values obtained by Smith (1998) and with the X-ray diffraction (XRD) measurements (10.6 Å) for Cs-vermiculite reported by Berend *et al.* (1995). The modeled value of ~10.4 Å for the interlayer spacing of dehydrated Na-montmorillonite is typical of the force field used (Boek *et al.*, 1995a; Chavez-Paez *et al.*, 2001b). The difference from the experimental value of ~9.6 Å (Berend *et al.*, 1995) may be attributed to the inability of the force field used to completely reproduce the system behavior for completely dehydrated states.

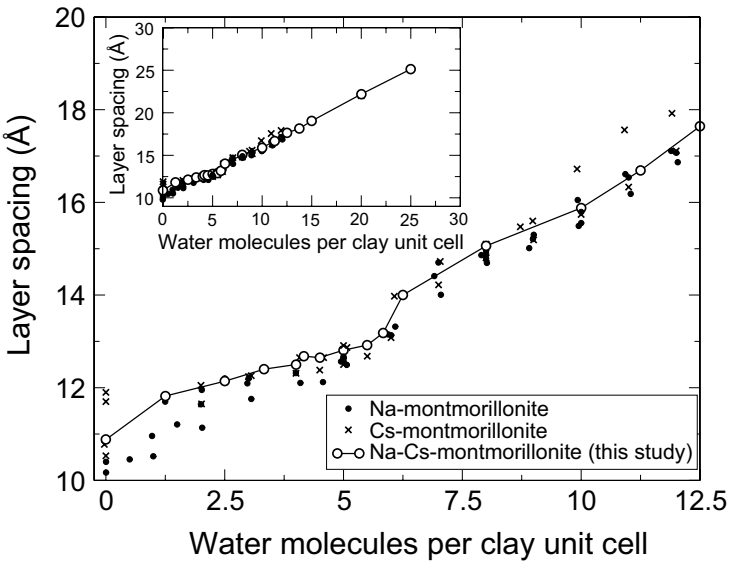

Figure 2. Swelling curves of the Na-Cs-montmorillonites investigated in comparison with those of pure Na- and Cs-montmorillonite from the authors' own calculations and from various other molecular modeling studies (Boek *et al.*, 1995a; Smith, 1998; Chavez-Paez *et al.*, 2001b; Marry and Turq, 2002; Marry *et al.*, 2002a; Malikova *et al.*, 2004a). Typical variations in the interlayer distance during the Monte Carlo simulations are ±0.5Å.

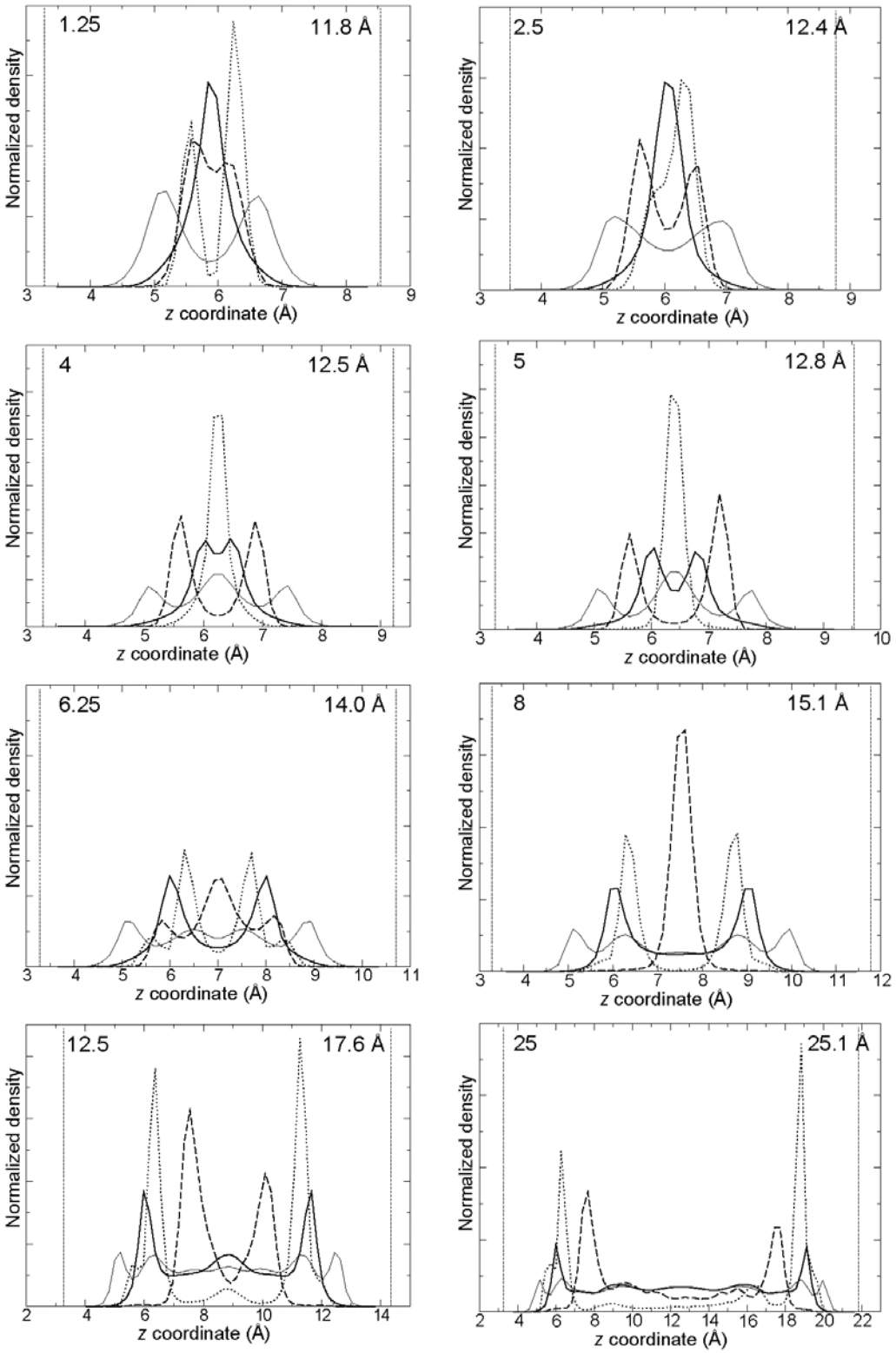

Figure 3. Normalized density profiles for O, H, Na^+, and Cs^+ at different interlayer water contents (water molecules per clay unit cell). Thick continuous lines denote O; thin continuous lines denote H; dashed lines denote Na^+; and dotted lines denote Cs^+. The numbers in the upper left corners correspond to interlayer water molecules per clay unit cell and in the upper right corners the interlayer spacings are indicated. The dotted vertical lines mark the position of the outermost oxygen on the basal plane of the clay sheet.

Structural properties of the interlayer

Interlayer density profiles for the hetero-ionic Na-Cs-montmorillonite are presented in Figure 3. For small interlayer water contents (monolayer or less), the oxygen sites of water molecules are always positioned in the middle of the interlayer. With increasing water content, the probability density profile of oxygen splits into multiple peaks, corresponding to the monolayer (4−5 H_2O per clay unit cell), bilayer (8−10 H_2O per clay unit cell), trilayer (12−15 H_2O per clay unit cell), and multilayer state of the interlayer water.

At water contents below the monolayer state, Cs^+ ions tend to sink into the hexagonal cavities of the tetrahedral sheet. In the monolayer state, Cs^+ ions occupy the middle of the interlayer and with increasing water content, they tend to stay close to the tetrahedral sheet surface next to the first oxygen peak.

Na^+ shows different behavior; depending on the interlayer hydration, either inner-sphere or outer-sphere complexes are observed. For monolayer states or less, only inner-sphere complexes are possible due to restrictions in geometry. In these states, Na^+ is bound directly to the clay surface and stays at an equilibrium distance of ~2.4 ± 0.05 Å from the surface. Note that, unlike the behavior in homo-ionic Na-montmorillonite, the Na^+ ions are positioned on the boundaries of the hexagonal cavities. This leads to the peak splitting seen in the density profile of Figure 3 for the monohydrated state. The different behavior of Cs^+ and Na^+ is related to the fact that the interlayer distance of the hetero-ionic Na-Cs-montmorillonite is significantly larger than for a homo-ionic Na-montmorillonite as outlined in the previous section. In an optimal configuration, Na^+ is 6-fold coordinated by oxygen sites at distances of ~2.3 Å. For mixed clay with larger interlayer spacing this coordination can be achieved if Na^+ ions are positioned on the boundaries of the hexagonal cavities.

In the bilayer state (8 H_2O molecules per clay unit cell in Figure 3), both outer- and inner-sphere complexes are observed. As the water content increases, the outer-sphere complexes become dominant. The equilibrium distance to the surface for the outer-sphere complexes is 5.2±0.1 Å. Similar behavior of the peak positions of Na^+ and Cs^+ is known from other simulations of montmorillonite with octahedral substitutions (Sutton and Sposito, 2001; Marry and Turq, 2003; Tambach *et al.*, 2004a).

The structural properties of water in the interlayer obtained for pentalayer hydration (bottom right in Figure 3) are comparable to those reported by Ichikawa *et al.* (2004) for a Na-beidellite with a much larger interlayer water content (for an interlayer distance of 144 Å). In both cases there is only one peak for the water oxygens at the clay surfaces and the movement of the interlayer ion is restricted to the first two water layers close to the surfaces. We therefore believe that the pentalayer state modeled in this work is comparable to the situation at two outer surfaces of (disintegrated) clay stacks.

Hydration of Na^+ and Cs^+ in the interlayer

Radial distribution functions (rdf) and coordination numbers for Na^+ are presented in Figures 4 and 5, respectively. The parameters for the first and second coordination shells of Na^+ are summarized in Tables 6 and 7, respectively.

As water content increases, the coordination of Na^+ by oxygen in the first coordination shell converges towards 6 (Figure 5). For monolayer water content or less, both interlayer water oxygens and tetrahedral clay oxygens form the first coordination shell. At greater water contents, only the interlayer water oxygens contribute to the first coordination shell. The typical interatomic distance (Na−O) is then ~2.3 Å. The missing contribution of tetrahedral clay oxygens to the first

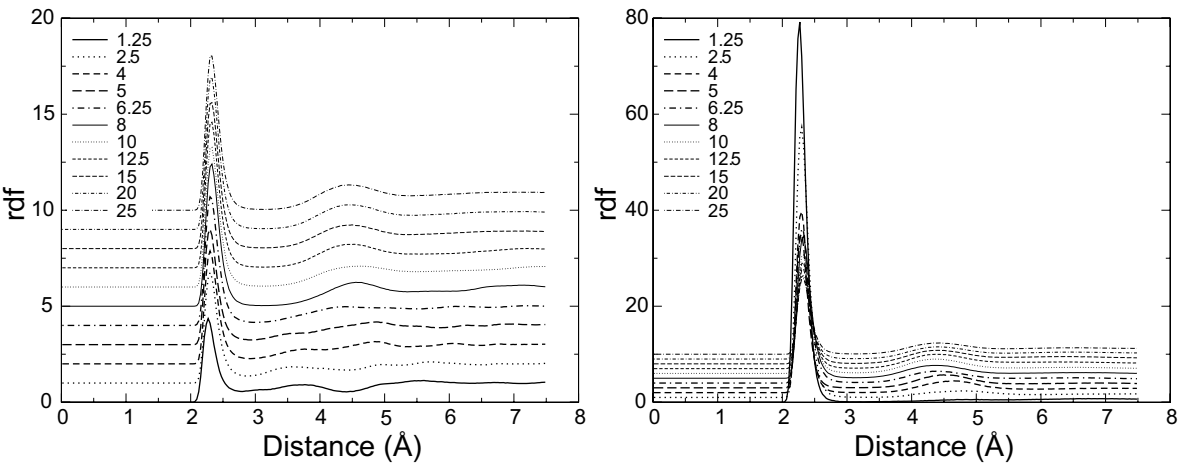

Figure 4. Stacked radial distribution functions (rdf) for Na−O, considering all oxygen atoms in the system (left) and oxygen from interlayer water only (right). The numbers correspond to interlayer water molecules per clay unit cell.

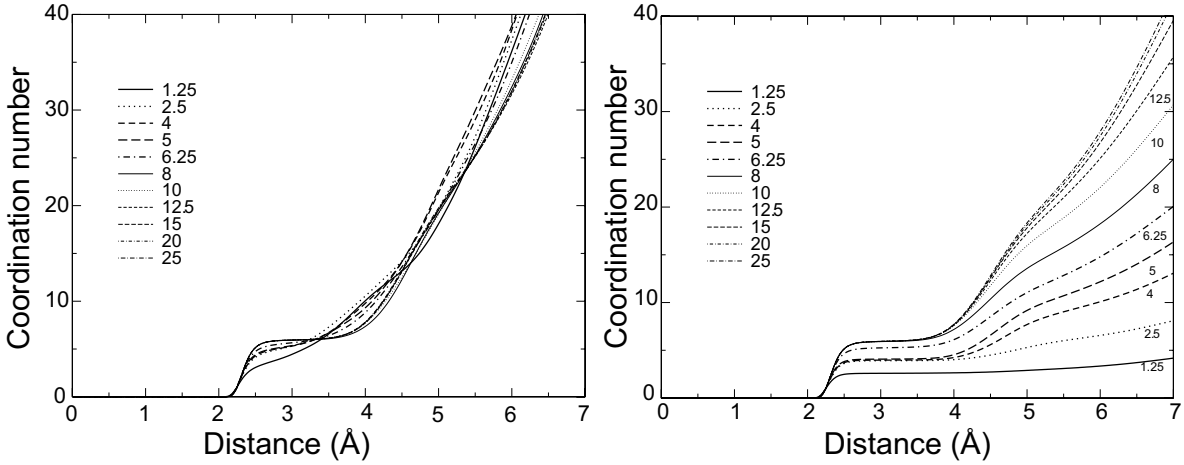

Figure 5. Coordination numbers for Na−O considering all oxygen atoms in the system (left) and oxygen from interlayer water only (right). The numbers correspond to interlayer water molecules per clay unit cell.

coordination shell of Na^+ at larger interlayer spacing indicates the formation of 'outer-sphere complexes' at the clay surfaces. The tetrahedral clay oxygens participate in the second coordination shell (see also Figure 3).

The Cs−O rdf at different hydration states and the corresponding coordination numbers are presented in Figures 6 and 7, respectively. The parameters of the first coordination shell of Cs^+ are summarized in Table 5. The position of the first peak of the Cs−O rdf (3.24 Å) is practically independent of the interlayer water content. Only at small interlayer water contents is the position of the first peak slightly greater. This is because at small water contents, more oxygen atoms from the tetrahedral sheets contribute to the first coordination shell than do water oxygens. According to the simulations (Table 5), the interatomic distance between Cs^+ and tetrahedral oxygens is larger than that between Cs^+ and water oxygens, therefore the first coordination peak is shifted to slightly greater values.

The average coordination number of Cs^+ by oxygen increases with hydration from 10 at near dry states to 11.8 for monolayer hydration. Further increase of hydration does not systematically change the coordination. For dry montmorillonite, Cs^+ is 12-fold coordinated with tetrahedral oxygens. Although the total coordination number is almost independent of water content, the relative contributions of the oxygen atoms from interlayer water and from tetrahedral sheets to the first coordination shell vary. For dry montmorillonite, there is obviously no contribution of water oxygens to the coordination shell. With increasing interlayer water content, the contribution of the water molecules to the first shell ($Cs-O_{water}$) increases asymptotically to 8.8 for the largest water content we have simulated. The contribution of tetrahedral oxygens ($Cs-O_{clay}$) decreases from 9 to 2.7 with increasing availability of interlayer water.

In a monohydrated system the $Cs-O_{water}$ interatomic distance is close to 3.2 Å and slightly larger $Cs-O_{clay}$ distances of 3.3−3.4 Å are observed (Table 5).

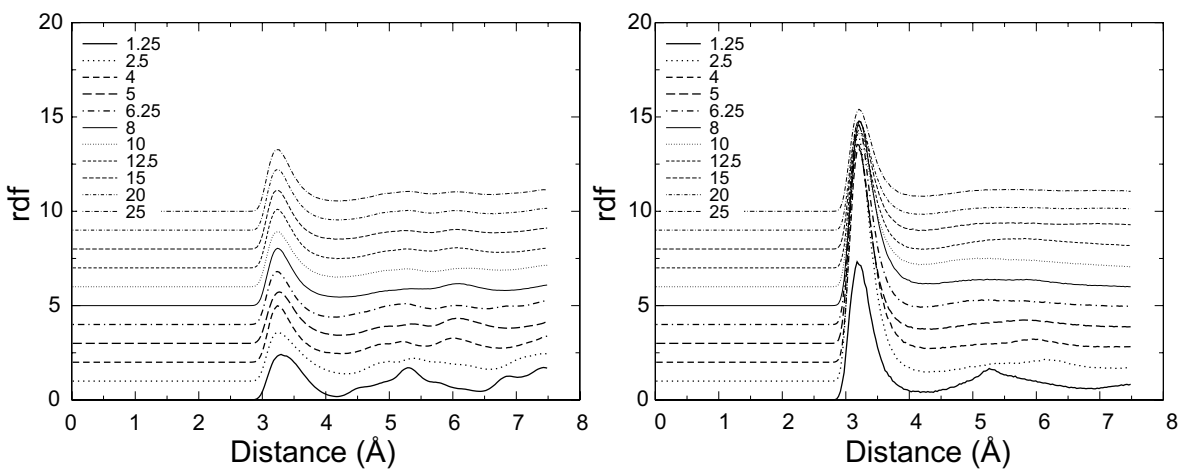

Figure 6. Stacked radial distribution functions (rdf) for Cs−O considering all oxygen atoms in the system (left) and oxygen from interlayer water only (right). The numbers correspond to interlayer water molecules per clay unit cell.

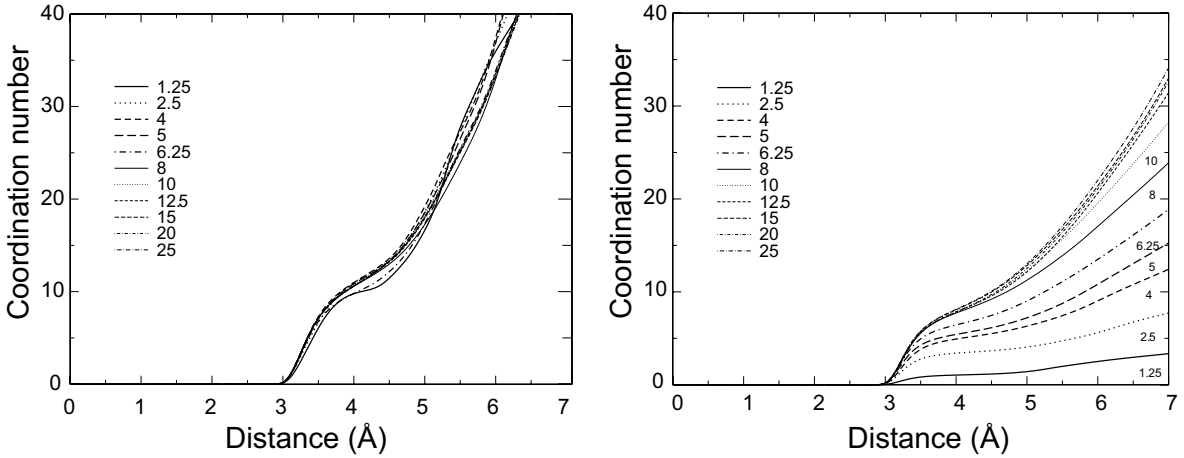

Figure 7. Coordination numbers of Cs−O considering all oxygen atoms in the system (left) and oxygen from interlayer water only (right). The numbers correspond to interlayer water molecules per montmorillonite unit cell.

The hydration behavior of Cs^+ and Na^+ in the interlayer of the mixed montmorillonite is in agreement with numerous classical molecular modeling studies, *i.e.* the running coordination numbers are very similar to those reported by Marry *et al.* (2002b, 2002c) who calculated a coordination number of 11.4 for monohydrated Cs-montmorillonite and 6.0 for monohydrated Na-montmorillonite. Nakano *et al*. (2003) investigated Cs sorbed on Kunipia-F bentonite, which contains 98−99% montmorillonite, by means of extended X-ray absorption fine structure spectroscopy and molecular modeling. They found an overall coordination number of 13.1 for Cs−O that can be separated into a contribution by interlayer water ($Cs-O_{water}$) of 7.4 and a contribution by tetrahedral oxygens ($Cs-O_{clay}$) of 5.69. Interatomic distances are 3.163 Å and 3.616 Å, respectively. The interatomic distances from our simulations are similar for $Cs-O_{water}$ and smaller for $Cs-O_{clay}$.

Sheet configuration for low hydration states

We investigated the configuration of the dry, mixed montmorillonite in order to have reference points for comparison with hydrated montmorillonite. In dry montmorillonite the first coordination shell of the interlayer ions is filled with oxygens from both tetrahedral sheets bounding the interlayer. Two configurations were found by analysis of XRD measurements on Cs-montmorillonite (Besson *et al.*, 1983; Berend *et al.*, 1995). The first configuration is a symmetric structure where the positions of hexagonal cavities of opposite clay layers coincide in the *a*,*b* plane. The Cs^+ ions are enclosed in the middle of the interlayer by the upper and lower hexagonal cavities. The second configuration is an asymmetric one, where a triangular site above a silicon atom of one clay layer is situated opposite a hexagonal cavity of the other layer. As discussed in detail later, intermediate configurations are also possible. Such an intermediate configuration was found by Telleria *et al.* (1977), using XRD measurements, on Ba-vermiculite. However, it should be noted that the TOT layers of vermiculite have a different structure from those of montmorillonite, due to the different charge distribution.

According to Smith (1998), the symmetric configuration is energetically favorable in a dry Cs-montmorillonite. In our simulations, the symmetric configuration is also the preferred configuration for the dehydrated Na-Cs-montmorillonite. This is reflected by

Table 5. Positions of the first maxima, R_{max}, and the first minima, R_{min}, of the Cs−O radial distribution function and the coordination numbers, *N,* of the first coordination shell for Cs^+ ions in the interlayer. The uncertainty in the positions of the minima and maxima is ±~0.03 Å.

Interlayer water per clay units	First coordination shell								
	R_{max} (Å)			R_{min} (Å)			*N*		
	$Cs-O_{all}$	$Cs-O_{clay}$	$Cs-O_{water}$	$Cs-O_{all}$	$Cs-O_{clay}$	$Cs-O_{water}$	$Cs-O_{all}$	$Cs-O_{clay}$	$Cs-O_{water}$
0 (dry)	3.25		–	4.2−4.35		–	12		–
1.25 (< monolayer)	3.30	3.3−3.4	3.18	4.17	4.18	4.17	10.0	9.0	1.0
5 (monolayer)	3.27	3.38	3.18	4.17	4.16	4.17−4.29	11.8	6.1	5.7
8 (bilayer)	3.24	3.36	3.21	4.23	4.23	4.2	11.5	3.1	8.4
25 (pentalayer)	3.24	3.36	3.21	4.2	4.21	4.23	11.5	2.7	8.8

Table 6. Positions of the first maxima, R_{max}, and the first minima, R_{min}, of the Na−O radial distribution function and the coordination numbers, N, of the first coordination shell for Na^+ ions in the interlayer. The uncertainty in the positions of the minima and maxima is ±~0.03 Å.

Interlayer water per clay units	First coordination shell								
	R_{max} (Å)			R_{min} (Å)			N		
	Na−O_{all}	Na−O_{clay}	Na−O_{water}	Na−O_{all}	Na−O_{clay}	Na−O_{water}	Na−O_{all}	Na−O_{clay}	Na−O_{water}
0 (dry)	2.4		–	2.8		–	3.4		–
1.25 (< monolayer)	2.27	2.45	2.27	2.80	2.80	3.12−3.24	3.7	2.4	1.0
5 (monolayer)	2.30	2.40	2.30	2.97	2.94	3.12−3.27	5.1	1.0	3.9
8 (bilayer)	2.33	–	2.33	3.09	–	3.09	5.8	0	5.8
25 (pentalayer)	2.30	–	2.30	3.15	–	3.12	5.9	0	5.9

the 12-fold coordination of Cs^+ with the tetrahedral oxygens (Table 5), whereas in an asymmetric structure, the Cs^+ ion is 9-fold coordinated with the tetrahedral oxygens. Weiss *et al.* (1990b) found both coordinations in Cs-exchanged dry clays. Also, the interlayer distance of 10.8±0.1 Å for the dehydrated Na-Cs-montmorillonite is similar to experimental values obtained for symmetric dry Cs-montmorillonites, *e.g.* Berend *et al.* (1995) report 10.7 Å for Cs-vermiculite in the symmetric and 11.5 Å in the asymmetric configuration. If water enters the interlayer at low hydration states, the sheet configuration changes to an asymmetric structure, which is expressed in the 9-fold coordination of Cs^+ with the tetrahedral oxygens and reduction of the overall coordination number (Table 5).

The interlayer distance and the sheet configuration of Na-Cs-montmorillonite can be interpreted as the result of a competition between the Na^+ and Cs^+ ions to fill their first coordination shell with sheet and interlayer water oxygens. The distance to the oxygens is quite different for the two ions (about a third greater for Cs^+ than for Na^+), therefore it is to be expected that Cs^+ will determine the sheet configuration for small interlayer distances and low hydration states.

Diffusion in the interlayer

In a first step we calculated the three-dimensional diffusion coefficient from interlayer species trajectories using equation 2. We chose a blocking length of 100 ps for calculation of the diffusion coefficients. This time interval is comparable to the characteristic time of measurements with quasielastic neutron scattering (QENS) techniques used for estimating water diffusion coefficients in clays (Malikova *et al.*, 2005; Rinnert *et al.*, 2005; Gonzalez *et al.*, 2007; Michot *et al.*, 2007). Malikova *et al.* (2005) found a very good quantitative agreement between QENS measurements and molecular modeling for mono- and bi-hydrated Na montmorillonite and for monohydrated Cs-montmorillonite. The 100 ps blocking period seems to give good results for diffusion coefficients at greater hydration states, but the time interval may be too short for reaching the asymptotic limits from equation 2 at low hydration states when the mobility of the interlayer species is strongly reduced. We therefore did longer runs, of up to 3.0 ns, for several hydration states and calculated directional diffusion coefficients D_{xx}, D_{yy}, and D_{zz}, based on these long trajectories, without averaging. We found that the diffusion coefficient perpendicular to the clay layers, D_{zz}, is at least one to two orders of magnitude less than in the other directions for the 100 ps blocking period, and close to zero for the long trajectories. This finding motivated us to transform the three-dimensional diffusion coefficients (100 ps blocking period) into two-dimensional ones, as described above. The two-dimensional diffusion coefficients for Cs^+, Na^+, and water in the interlayer are shown in Figure 8. Two-dimensional diffusion coefficients from the long runs are shown in

Table 7. Positions of the second maxima, R_{max}, and the second minima, R_{min}, of the Na−O radial distribution function and the coordination numbers, N, of the second coordination shell for Na^+ ions in the interlayer. The uncertainty in the positions of the minima and maxima is ±~0.03 Å.

Interlayer water per clay units	Second coordination shell								
	R_{max} (Å)			R_{min} (Å)			N		
	Na−O_{all}	Na−O_{clay}	Na−O_{water}	Na−O_{all}	Na−O_{clay}	Na−O_{water}	Na−O_{all}	Na−O_{clay}	Na−O_{water}
0 (dry)	4.5		–	4.55−4.7		–	14−16		–
1.25 (< monolayer)	3.76	3.76	4.7	4.41	4.39	5.5−5.6	12.4	9.8	2.8
5 (monolayer)	4.85	3.6	4.5	5.93	4.3	5.79	26.5	6.7	10.7
8 (bilayer)	4.60	4.65	4.40	5.35	5.29	5.52	23	8	15
25 (pentalayer)	4.45	–	4.36	5.41	5.35	5.41	24	2.3	22

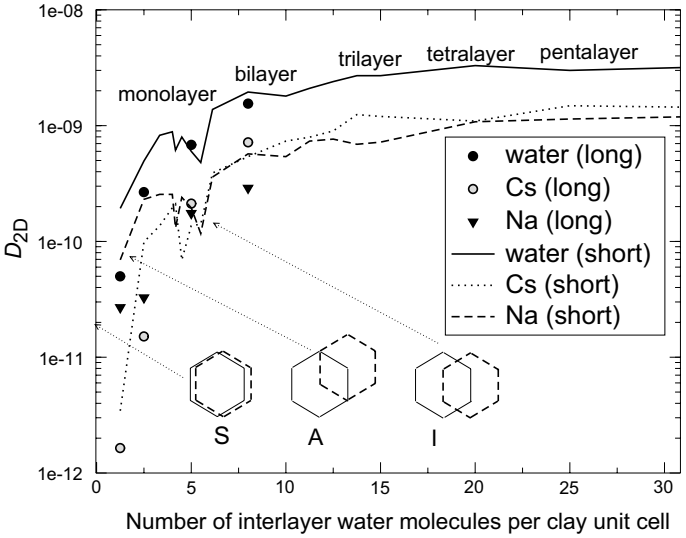

Figure 8. Absolute two-dimensional diffusion coefficients of interlayer ions and water in mixed Na-Cs-montmorillonite for short and long simulations calculated as a function of water content with the OPLS-TIP4P force field (see text). A sketch of the three limiting positions of each layer surface towards the opposite one is inserted in the lower half of the figure. Each sheet is represented by only one hexagonal structure. The symmetric structure is denoted by S, the asymmetric by A and the intermediate one by I. The arrows indicate at which water content the structures occur.

addition, for selected hydration states. These values were obtained from the one-dimensional, directional diffusion coefficients, by averaging D_{xx} and D_{yy}. Diffusion coefficients change in a very non-linear way with increasing water content. For monolayer water contents or less, the absolute value of the diffusion coefficient for Cs^+ is less than for Na^+. If the interlayer water contents increase, the diffusion coefficient of Cs^+ becomes slightly larger than for Na^+. Note that for ⅓ monolayer and ⅔ monolayer hydration the diffusion coefficients calculated from the long trajectories are systematically lower than the corresponding values for the shorter trajectories. A visual inspection of interlayer species' trajectories at different hydration states revealed that for the ⅓ monolayer and ⅔ monolayer hydrates, the mobility of the interlayer species is very much restricted. The Cs^+ ions, in particular, but also some Na^+ ions, and water molecules, remain fixed to their positions throughout the duration of the simulations. The Cs^+ and Na^+ tend to stay in the center of tetrahedral rings and oscillate around their position, whereas water molecules are shared between cations for several hundred picoseconds. As a consequence, diffusion coefficients calculated from the 100 ps averaged trajectories represent the mobility around a fixed position, whereas those calculated from the long trajectories are related to the probability that they leave such a position. Note that for ⅓ monolayer hydration, for example, we did not observe a single Cs^+ leaving its position, even in the longer simulations. These findings are in accord with the results of Sutton and Sposito (2002) who found a non-linear decrease in the diffusion coefficient with simulation time, especially for ⅓ monohydrated Cs-montmorillonite, and observed a very similar behavior of the interlayer species. Based on this observation we conclude that QENS measurements of water diffusion in little-hydrated Cs-montmorillonite probably overestimate the mobility of water (compared with macroscopic diffusion experiments).

Figure 9 shows the relative diffusion coefficients of Cs^+, Na^+, and water as a function of interlayer water content, providing a qualitative picture of reduced mobility in the interlayer. The values for monolayer, bilayer, trilayer, and pentalayer water are summarized in Table 8. If diffusion in the interlayer is similar to diffusion in bulk water, the relative diffusion coefficient is ~1. For Na^+, the relative diffusion coefficient is only slightly less than for water and shows the same increase with increasing water contents. The absolute values for interlayer diffusion coefficients were calculated as two-dimensional diffusion coefficients in the *xx,yy* plane using equation 2 and can be compared directly to three-dimensional diffusion coefficients in bulk water. The relative diffusion coefficients for Na^+ and water reach one at greater water content. On a sufficiently long timescale the rate of diffusive transport of Na^+ and water is comparable to diffusion in bulk water.

The relative diffusion coefficient of Cs^+ also increases with increasing water content, but it is always significantly less than those of water and Na (note that in bulk water, Cs^+ diffuses ~50% faster than Na^+, see Table 8). This reflects the reduced mobility of the Cs^+ ions due to their binding to the clay surface as inner-sphere complexes. At very small water contents, the relative diffusion coefficient of Cs^+ is ~10 times smaller than for Na^+ and water, as the Cs^+ ions tend to become

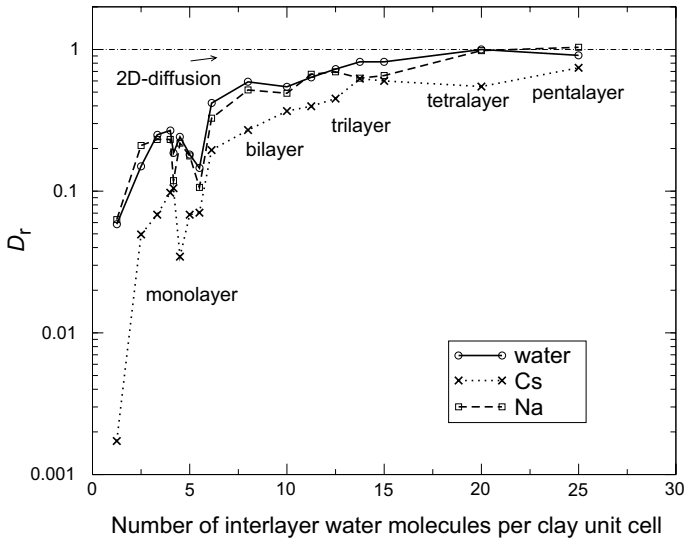

Figure 9. Relative diffusion coefficients (equation 3) of interlayer ions and water in mixed Na-Cs-montmorillonite calculated as a function of water content with the OPLS-TIP4P force field.

immobilized in the hexagonal cavities of the tetrahedral sheet. This finding is supported by the EXAFS measurements of Kemner *et al.* (1997), who found that the Cs ions in smectite are in a more disordered environment in expanded layers (*i.e.* the Cs ions being loosely associated with a single ditrigonal cavity at the clay surface).

The simulations by Sutton and Sposito (2001) showed two distinct Cs^+ species at ⅔ monolayer hydration (corresponds to 2.5−3 water per clay unit), one which shows oscillatory movement, and another which exhibits diffusional behavior.

The diffusion of Na^+ and Cs^+ in the interlayer of bihydrated montmorillonite was also investigated by Marry and Turq (2003) using the SPC/E-water model (Table 5). The main difference from our simulations is that theirs were based on a Na-montmorillonite with a single Na^+ atom replaced by Cs^+. The relative diffusion coefficients for Na^+ and water are comparable with those which we obtained, whereas the values for Cs^+ are slightly greater. The Cs^+ values are based on the simulations of one Cs^+ ion in a Na-montmorillonite, therefore the difference might be attributed to the different system setup and maybe also partly to the different force field parameters. Despite the small differences, the general trend is the same.

Nevertheless, the relative diffusion coefficients for Cs^+ ions from this work and other molecular dynamics simulations are ~20 times greater than that of Bourg *et al.* (2006) obtained from diffusion experiments. In order to derive interlayer diffusion coefficients from experiments, several assumptions have to be made about pore-size distributions, water distribution between voids and interlayer, sorption in the interlayer and on edge sites, as well as the kinetics and sorption mechanisms. A change in any of these assumptions may result in substantial differences in the interlayer diffusion coefficients obtained. Deeper understanding of Cs^+ transport in clays is needed to resolve such discrepancies.

For monolayer water content, we found a significant reduction of the diffusion coefficients for all interlayer species, with the smallest values at a water content of 5−5.5 H_2O per clay unit cell. The reduction is accompanied by a slow increase in the interlayer spacing:

Table 8. Relative diffusion coefficients extracted from Figure 9.

D_i/D_0	Monolayer (4−5 water molecules per clay unit cell)	Bilayer (8−10 water molecules per clay unit cell)	Bilayer (Marry and Turq, 2003; Bourg, 2004)	Trilayer (12−15 water molecules per clay unit cell)	Tetralayer (20 water molecules per clay unit cell)	Pentalayer (25 water molecules per clay unit cell)
Cs^+	0.035−0.11	0.27−0.38	0.63±0.26	0.45−0.63	0.55	0.75
Na^+	0.12−0.24	0.5−0.53	0.57±0.21	0.62−0.71	0.98	1.04
H_2O	0.15−0.27	0.54−0.59	0.6±0.12	0.72−0.81	1.01	0.92

Data from Bourg (2004) for water represent averaged values from different experiments and molecular modeling studies. The data of Marry and Turq (2003) for Cs^+ and Na^+ are based on molecular modeling simulations.

the diffusion coefficient for a water content of 5.5 H_2O per clay unit cell is comparable to that at a water content of 2.5 H_2O per clay unit cell, but the interlayer spacings are 12.14 Å and 12.92 Å, respectively. We think that the reduction of the diffusion coefficient is related to the change in the sheet configuration of the mixed montmorillonite. At a water content of three water molecules per clay unit cell, we found a nearly perfect asymmetric sheet configuration. With increasing water content, the orientation of adjacent TOT layers changes to an intermediate configuration between asymmetric and symmetric. We found displacements between adjacent sheets close to $\pm b/4$. Marry *et al.* (2002a) reported that such an intermediate configuration was preferred for a monohydrated montmorillonite when Na^+ was the counterion. Experimental studies support the principal occurrence of such configurations, *e.g.* Telleria *et al.* (1977) which reported a displacement of $\pm b/4$ on adjacent silicate sheets for a Ba-vermiculite.

The different configurations in our simulations, symmetric (S) at dry conditions, asymmetric (A) at very small water contents, and intermediate (I) at a monohydrated state, are sketched in the lower half of Figure 8. The intermediate state shows smaller diffusion coefficients than the asymmetric one, although the interlayer distance is greater for the intermediate state. Marry *et al*. (2002a) described such an intermediate configuration as the preferred one for a monohydrated Na-montmorillonite. They also found that interlayer diffusion coefficients depend on the configuration, for both Na- and Cs-montmorillonite.

For bilayer water content or more, the competitive effects on the sheet configuration are negligible, as enough room and water is available to optimize the first coordination shell for both ions.

SUMMARY

We investigated the dynamics of water and cations in the interlayer of a mixed Na-Cs-montmorillonite as a function of the interlayer water content. It is the first time that such a mixed Na-Cs-montmorillonite has been investigated using Monte Carlo and classical, molecular-dynamics methods. The study focused on the structure of the water-clay interface and on diffusion processes in the interlayer. We used idealized clay models without considering interstratifications, non-uniform hydration, or water adsorption-desorption hysteresis. The swelling behavior of mixed Na-Cs-montmorillonite is comparable with that found in previous numerical and experimental studies on pure Cs- and Na-montmorillonite. For a dry configuration of mixed montmorillonite we found that, similar to pure Cs-montmorillonite (Smith, 1998), a symmetric structure is preferred. This can be attributed to a competition between Na^+ and Cs^+ filling their coordination shells with oxygen atoms from the TOT layer. The bond lengths are much greater for Cs–O than for Na–O, therefore Cs^+ coordination chemistry governs the relative configuration of TOT layers at small water contents.

We found that Cs^+ in the interlayer is preferentially bound to the tetrahedral sheet surface in the form of inner-sphere complexes, whereas Na^+ is bound as an outer sphere complex, if the interlayer distance allows this. Sutton and Sposito (2001) also carried out an extensive comparison and discussion of their modeling results for Cs-smectite hydrates with the ^{133}Cs-NMR data from Kim *et al.* (1996a, 1996b) and Weiss *et al.* (1990b, 1990a). They found some disagreement between their simulations and the nuclear magnetic resonance data, and concluded that there is need for further NMR studies which control layer spacing and take into account the effects of microporosity in Cs-smectites.

The diffusion behavior of water and Na^+ is very similar at all hydration states. Their relative diffusion coefficients increase with hydration and level off at tetralayer and higher hydration states to values that correspond to unretarded diffusion in a two-dimensional domain.

The absolute diffusion coefficients of Cs^+ are equal to or even greater than those of Na^+ for more than monolayer water contents. This seems reasonable, taking into account that Cs^+ has a greater diffusion coefficient than Na^+ in bulk water (Table 4). The relative diffusion coefficient of Cs^+ is less than those of Na^+ and water at all hydration states. At very low hydration, Cs^+ ions become immobilized due to their tendency to sink into hexagonal cavities of the clay tetrahedral sheets. At high hydration states the values of the relative diffusion coefficient for Cs^+ are less than for water and Na^+, because the formation of inner-sphere complexes and the strong interaction with the surface reduce the mobility of the Cs^+ ions.

The values for the diffusion coefficients of Na^+ and Cs^+ in monohydrated and bihydrated interlayers are also in the same range as values obtained in other molecular-dynamics studies. Perfect agreement cannot be expected, since such values are dependent on the force fields used and on the positioning of tetrahedral and octahedral substitutions. For monolayer water, we observed a local minimum for the diffusion coefficients. This can be attributed to a shift in the configuration of clay layers bounding the interlayer. A similar dependency of diffusion coefficients on the layer configuration is reported by Marry *et al.* (2002a) for monohydrated Na- and Cs-montmorillonite.

The values for the relative diffusion coefficients of Cs^+ extracted from our simulations are smaller than those obtained in previous studies (Marry and Turq, 2003; Bourg, 2004), but they are still ~20 times larger than relative diffusion coefficients derived from experiments (Bourg, 2004). The reason for this is not clear and indicates some lack of mechanistic understanding in the diffusion of Cs^+ in the interlayers of clays.

ACKNOWLEDGMENTS

The simulations were performed on PSI's MERLIN cluster and on the HORIZON in the CSCS-Manno. Special thanks go to Neal Skipper for his help with the Monte Carlo modeling and for fruitful discussions. The work was partially financed by the Swiss National Cooperative for the Disposal of Radioactive Waste (Nagra). Associate editor, Will Gates, and Bruno Lanson and two other anonymous reviewers are thanked for their detailed and constructive comments.

REFERENCES

Arab, M., Bougeard, D., and Smirnov, K.S. (2003) Structure and dynamics of the interlayer water in an uncharged 2:1 clay. *Physical Chemistry Chemical Physics*, **5**, 4699–4707.

Arab, M., Bougeard, D., and Smirnov, K.S. (2004) Structure and dynamics of interlayer species in a hydrated Zn-vermiculite. A molecular dynamics study. *Physical Chemistry Chemical Physics*, **6**, 2446–2453.

Berend, I., Cases, J.M., Francois, M., Uriot, J.P., Michot, L., Masion, A., and Thomas, F. (1995) Mechanism of adsorption and desorption of water-vapor by homoionic montmorillonites. 2. The Li^+, Na^+, K^+, Rb^+ and Cs^+-exchanged forms. *Clays and Clay Minerals*, **43**, 324–336.

Besson, G., Glaeser, R., and Tchoubar, C. (1983) Cesium – a means of determining the structure of smectites. *Clay Minerals*, **18**, 11–19.

Boek, E.S. and Sprik, M. (2003) Ab initio molecular dynamics study of the hydration of a sodium smectite clay. *Journal of Physical Chemistry B*, **107**, 3251–3256.

Boek, E.S., Coveney, P.V., and Skipper, N.T. (1995a) Monte Carlo molecular modeling studies of hydrated Li-, Na-, and K-smectites: Understanding the role of potassium as a clay swelling inhibitor. *Journal of the American Chemical Society*, **117**, 12608–12617.

Boek, E.S., Coveney, P.V., and Skipper, N.T. (1995b) Molecular modeling of clay hydration: A study of hysteresis loops in the swelling curves of sodium montmorillonites. *Langmuir*, **11**, 4629–4631.

Bourg, I.C. (2004) Tracer diffusion of water and inorganic ions in compacted saturated sodium bentonite. PhD thesis, University of California, Berkeley, 368 pp.

Bourg, I.C., Bourg, A.C.M., and Sposito, G. (2003) Modeling diffusion and adsorption in compacted bentonite: A critical review. *Journal of Contaminant Hydrology*, **61**, 293–302.

Bourg, I.C., Sposito, G., and Bourg, A.C.M. (2006) Tracer diffusion in compacted, water-saturated bentonite. *Clays and Clay Minerals*, **54**, 363–374.

Bradbury, M.H. and Baeyens, B. (2000) A generalized sorption model for the concentration dependent uptake of cesium by argillaceous rocks. *Journal of Contaminant Hydrology*, **42**, 141–163.

Brigatti, M.F., Galán, E., and Theng, B.K.G. (2006) Structures and mineralogy of clay minerals. Pp. 19–68 in: *Handbook of Clay Science* (F. Bergaya, B.K.G. Theng, and G. Lagaly, editors). Developments in Clay Science, **1**, Elsevier, Amsterdam.

Calvet, R. (1973) Hydration of montmorillonite and diffusion of exchangeable cations. 2. Diffusion of exchangeable cations in montmorillonite. *Annales Agronomiques*, **24**, 135–217.

Chavez-Paez, M., de Pablo, L., and de Pablo, J.J. (2001a) Monte Carlo simulations of Ca-montmorillonite hydrates. *Journal of Chemical Physics*, **114**, 10948–10953.

Chavez-Paez, M., Van Workum, K., de Pablo, L., and de Pablo, J.J. (2001b) Monte Carlo simulations of Wyoming sodium montmorillonite hydrates. *Journal of Chemical Physics*, **114**, 1405–1413.

Cygan, R.T., Liang, J.-J., and Kalinichev, A.G. (2004) Molecular models of hydroxide, oxyhydroxide, and clay phases and the development of a general force field. *Journal of Physical Chemistry B*, **108**, 1255–1266.

de Carvalho, R.J.F.L. and Skipper, N.T. (2001) Atomistic computer simulation of the clay-fluid interface in colloidal laponite. *Journal of Chemical Physics*, **114**, 3727–3733.

Deer, W.A., Howie, R.A., and Zussman, J. (1992) *An Introduction to the Rock-Forming Minerals*. Longman Scientific & Technical, Harlow, Essex, England, 712 pp.

Ferrage, E., Lanson, B., Sakharov, B.A., and Drits, V.A. (2005) Investigation of smectite hydration properties by modeling experimental X-ray diffraction patterns: Part I. Montmorillonite hydration properties. *American Mineralogist*, **90**, 1358–1374.

Ferrage, E., Lanson, B., Sakharov, B.A., Geoffroy, N., Jacquot, E., and Drits, V.A. (2007) Investigation of dioctahedral smectite hydration properties by modeling of X-ray diffraction profiles: Influence of layer charge and charge location. *American Mineralogist*, **92**, 1731–1743.

Flury, M. and Gimmi, T. (2002) Solute diffusion. Pp. 1323–1351 in: *Methods of Soil Analysis, Part 4 – Physical Methods* (J.H. Dane and G.C. Topp, editors). Soil Science Society of America, Madison, Wisconsin, USA.

Flyvbjerg, H. and Petersen, H.G. (1989) Error-estimates on averages of correlated data. *Journal of Chemical Physics*, **91**, 461–466.

Fu, M.H., Zhang, Z.Z., and Low, P.F. (1990) Changes in the properties of a montmorillonite-water system during the adsorption and desorption of water – hysteresis. *Clays and Clay Minerals*, **38**, 485–492.

Gonzalez, F., Juranyi, F., Van Loon, L., and Gimmi, T. (2007) Translational diffusion of water in compacted clay systems. *European Physical Journal-Special Topics*, **141**, 65–68.

Greathouse, J.A., Refson, K., and Sposito, G. (2000) Molecular dynamics simulation of water mobility in magnesium-smectite hydrates. *Journal of the American Chemical Society*, **122**, 11459–11464.

Hensen, E.J.M. and Smit, B. (2002) Why clays swell. *Journal of Physical Chemistry B*, **106**, 12664–12667.

Hensen, E.J.M., Tambach, T.J., Bliek, A., and Smit, B. (2001) Adsorption isotherms of water in Li-, Na-, and K-montmorillonite by molecular simulation. *Journal of Chemical Physics*, **115**, 3322–3329.

Ichikawa, Y., Kawamura, K., Theramast, N., and Kitayama, K. (2004) Secondary and tertial consolidation of bentonite clay: Consolidation test, molecular dynamics simulation and multiscale homogenization analysis. *Mechanics of Materials*, **36**, 487–513.

Iwasaki, T. and Watanabe, T. (1988) Distribution of Ca and Na ions in dioctahedral smectites and interstratified dioctahedral mica smectites. *Clays and Clay Minerals*, **36**, 73–82.

Jorgensen, W.L. and Tirado-Rives, J. (1988) The OPLS (optimized potentials for liquid simulations) potential functions for proteins, energy minimizations for crystals of cyclic peptides and crambin. *Journal of the American Chemical Society*, **110**, 1657–1666.

Jorgensen, W.L., Chandrasekhar, J., and Madura, J.D. (1983) Comparison of simple potential functions for simulating liquid water. *Journal of Chemical Physics*, **79**, 926–935.

Kawamura, K., Ichikawa, Y., Nakano, M., Kitayama, K., and Kawamura, H. (1999) Swelling properties of smectite up to 90 degrees C – in situ X-ray diffraction experiments and molecular dynamic simulations. *Engineering Geology*, **54**, 75–79.

Kemner, K.M., Hunter, D.B., Bertsch, P.M., Kirkland, J.P., and Elam, W.T. (1997) Determination of site specific binding environments of surface sorbed cesium on clay minerals by

Cs-EXAFS. *Journal de Physique IV*, **7**, C2.777–C2.779.
Kim, Y., Cygan, R.T., and Kirkpatrick, R.J. (1996a) Cs-133 NMR and XPS investigation of cesium adsorbed on clay minerals and related phases. *Geochimica et Cosmochimica Acta*, **60**, 1041–1052.
Kim, Y., Kirkpatrick, R.J., and Cygan, R.T. (1996b) Cs-133 NMR study of cesium on the surfaces of kaolinite and illite. *Geochimica et Cosmochimica Acta*, **60**, 4059–4074.
Laird, D.A. (2006) Influence of layer charge on swelling of smectites. *Applied Clay Science*, **34**, 74–87.
Mahoney, M.W. and Jorgensen, W.L. (2001) Diffusion constant of the TIP5P model of liquid water. *Journal of Chemical Physics*, **114**, 363–366.
Malikova, N., Marry, V., Dufreche, J.F., and Turq, P. (2004a) Na/Cs montmorillonite: Temperature activation of diffusion by simulation. *Current Opinion in Colloid and Interface Science*, **9**, 124–127.
Malikova, N., Marry, V., Dufreche, J.F., Simon, C., Turq, P., and Giffaut, E. (2004b) Temperature effect in a montmorillonite clay at low hydration – microscopic simulation. *Molecular Physics*, **102**, 1965–1977.
Malikova, N., Cadene, A., Marry, V., Dubois, E., Turq, P., Zanotti, J.M., and Longeville, S. (2005) Diffusion of water in clays – microscopic simulation and neutron scattering. *Chemical Physics*, **317**, 226–235.
Marry, V. and Turq, P. (2002) Microscopic simulations of interlayer structure and dynamics in bihydrated heteroionic montmorillonites. *Journal of Chemical Physics*, **117**, 3454–3463.
Marry, V. and Turq, P. (2003) Microscopic simulations of interlayer structure and dynamics in bihydrated heteroionic montmorillonites. *Journal of Physical Chemistry B*, **107**, 1832–1839.
Marry, V., Turq, P., Cartailler, T., and Levesque, D. (2002a) Microscopic simulation of structure and dynamics of water and counterions in a monohydrated montmorillonite. *Journal of Chemical Physics*, **117**, 3454–3463.
Marry, V., Dufreche, J.F., Jardat, M., Meriguet, G., Turq, P., and Grun, F. (2002b) Dynamics and transport in charged porous media. *Colloids and Surfaces A – Physicochemical and Engineering Aspects*, **222**, 147–153.
Marry, V., Grun, F., Simon, C., Jardat, M., Turq, P., and Amatore, C. (2002c) Structure and dynamics in colloidal and porous charged media. *Journal of Physics: Condensed Matter*, **14**, 9207–9221.
Michot, L.J., Bihannic, I., Pelletier, M., Rinnert, E., and Robert, J.L. (2005) Hydration and swelling of synthetic Na-saponites: Influence of layer charge. *American Mineralogist*, **90**, 166–172.
Michot, L.J., Delville, A., Humbert, B., Plazanet, M., and Levitz, P. (2007) Diffusion of water in a synthetic clay with tetrahedral charges by combined neutron time-of-flight measurements and molecular dynamics simulations. *Journal of Physical Chemistry C*, **111**, 9818–9831.
Mooney, R.W., Keenan, A.G., and Wood, L.A. (1952) Adsorption of water vapor by montmorillonite. 2. Effect of exchangeable ions and lattice swelling as measured by X-ray diffraction. *Journal of the American Chemical Society*, **74**, 1371–1374.
Nagra (2002) *Project Opalinus Clay: Safety report*. Nagra Technical Report **02-05**, Nagra, Wettingen, Switzerland, 718 pp.
Nakano, M., Kawamura, K., and Ichikawa, Y. (2003) Local structural information of Cs in smectite hydrates by means of an EXAFS study and molecular dynamics simulations. *Applied Clay Science*, **23**, 15–23.
Norrish, K. (1954) The swelling of montmorillonite. *Discussions of the Faraday Society*, **18**, 120–134.
Norrish, K. and Quirk, J.P. (1954) Crystalline swelling of montmorillonite – use of electrolytes to control swelling. *Nature*, **173**, 255–256.
Pons, C.H., Rousseaux, F., and Tchoubar, D. (1981) Use of low-angle scattering from a synchrotron-beam for studying the swelling of smectites. 1. Study of the water-montmorillonite-sodium system as a function of temperature. *Clay Minerals*, **16**, 23–42.
Prayongphan, S., Ichikawa, Y., Kawamura, K., Suzuki, S., and Chae, B.G. (2006) Diffusion with micro-sorption in bentonite: Evaluation by molecular dynamics and homogenization analysis. *Computational Mechanics*, **37**, 369–380.
Reddy, M.R. and Berkowitz, M. (1988a) Conductance of Cs^+ ion in water – molecular-dynamics simulation. *Journal of Solution Chemistry*, **17**, 1183–1191.
Reddy, M.R. and Berkowitz, M. (1988b) Temperature-dependence of conductance of the Li^+, Cs^+, and Cl^- ions in water – molecular-dynamics simulation. *Journal of Chemical Physics*, **88**, 7104–7110.
Rinnert, E., Carteret, C., Humbert, B., Fragneto-Cusani, G., Ramsay, J.D.F., Delville A., Robert, J.L., Bihannic, I., Pelletier, M., and Michot, L.J. (2005) Hydration of a synthetic clay with tetrahedral charges: A multidisciplinary experimental and numerical study. *Journal of Physical Chemistry B*, **109**, 23745–23759.
Sainz-Díaz, C.I., Timón, V., Totella, V., Artacho, E., and Hernández-Laguna, A. (2002) Quantum mechanical calculations of dioctahedral 2:1 phyllosilicates: Effect of octahedral cation distributions in pyrophyllite, illite, and smectite. *American Mineralogist*, **87**, 958–965.
Skipper, N.T., Refson, K., and McConnell, J.D.C. (1991) Computer-simulation of interlayer water in 2-1 clays. *Journal of Chemical Physics*, **94**, 7434–7445.
Skipper, N.T., Sposito, G., and Chang, F.R.C. (1995a) Monte-Carlo simulation of interlayer molecular-structure in swelling clay minerals. 2. Monolayer hydrates. *Clays and Clay Minerals*, **43**, 294–303.
Skipper, N.T., Chang, F.R.C., and Sposito, G. (1995b) Monte-Carlo simulation of interlayer molecular-structure in swelling clay-minerals. 1. Methodology. *Clays and Clay Minerals*, **43**, 285–293.
Skipper, N.T., Lock, P.A., Titiloye, J.O., Swenson, J., Mirza, Z.A., Howells, W.S., and Fernandez-Alonso, F. (2006) The structure and dynamics of 2-dimensional fluids in swelling clays. *Chemical Geology*, **230**, 182–196.
Slade, P.G., Quirk, J.P., and Norrish, K. (1991) Crystalline swelling of smectite samples in concentrated NaCl solutions in relation to layer charge. *Clays and Clay Minerals*, **39**, 234–238.
Smith, D.E. (1998) Molecular computer simulations of the swelling properties and interlayer structure of cesium montmorillonite. *Langmuir*, **14**, 5959–5967.
Smith, W. and Forester, T.R. (1996) DL_POLY_2.0: A general-purpose parallel molecular dynamics simulation package. *Journal of Molecular Graphics*, **14**, 136–141.
Smith, W., Yong, C.W., and Rodger, P.M. (2002) DL_POLY: Application to molecular simulation. *Molecular Simulation*, **28**, 385–471.
Sutton, R. and Sposito, G. (2001) Molecular simulation of interlayer structure and dynamics in 12.4 angstrom Cs-smectite hydrates. *Journal of Colloid and Interface Science*, **237**, 174–184.
Sutton, R. and Sposito, G. (2002) Animated molecular dynamics simulations of hydrated caesium-smectite interlayers. *Geochemical Transactions*, **3**, 73–80.
Tambach, T.J., Hensen, E.J.M., and Smit, B. (2004a) Molecular simulations of swelling clay minerals. *Journal of Physical Chemistry B*, **108**, 7586–7596.
Tambach, T.J., Bolhuis, P.G., and Smit, B. (2004b) A

molecular mechanism of hysteresis in clay swelling. *Angewandte Chemie-International Edition*, **43**, 2650–2652.

Telleria, M.I., Slade, P.G., and Radoslovich, E.W. (1977) X-ray study of interlayer region of a barium-vermiculite. *Clays and Clay Minerals*, **25**, 119–125.

Teppen, B.J. and Miller, D.M. (2006) Hydration energy determines isovalent cation exchange selectivity by clay minerals. *Soil Science Society of America Journal*, **70**, 31–40.

Van Loon, L.R. and Jakob, A. (2005) Evidence for a second transport porosity for the diffusion of tritiated water (HTO) in a sedimentary rock (Opalinus Clay – OPA): Application of through- and out-diffusion techniques. *Transport in Porous Media*, **61**, 193–214.

Weiss, C.A., Kirkpatrick, R.J., and Altaner, S.P. (1990a) The structural environments of cations adsorbed onto clays – Cs-133 variable-temperature MAS NMR spectroscopic study of hectorite. *Geochimica et Cosmochimica Acta*, **54**, 1655–1669.

Weiss, C.A., Kirkpatrick, R.J., and Altaner, S.P. (1990b) Variations in interlayer cation sites of clay-minerals as studied by Cs-133 MAS nuclear-magnetic-resonance spectroscopy. *American Mineralogist*, **75**, 970–982.

(*Received 18 May 2007; revised 17 December 2007; Ms. 0030; A.E. W.P. Gates*)